Korean J. Chem. Eng., **30**(3), 751-760 (2013)
DOI: 10.1007/s11814-012-0186-x

Preparation and characterization of dimethyldichlorosilane modified SiO_2/PSf nanocomposite membrane

Majid Pakizeh*,†, Amir Neghad Moghadam*, Mohammad Reza Omidkhah, and Mahdieh Namvar-Mahboub***

*Department of Chemical Engineering, Faculty of Engineering, Ferdowsi University of Mashhad, P. O. Box 9177948974, Mashhad, Iran
**Department of Chemical Engineering, Faculty of Engineering, Tarbiat Modaress University, Tehran, Iran
(*Received 7 June 2012 • accepted 3 November 2012*)

Abstract−Investigations on nanocomposite membranes imply that these hybrid materials recommend promising new-generation membranes for gas separation in future. In this study, to investigate the effects of preparation parameters on the morphology and gas transport, various parameters including nanofiller content, surface modification and polymer concentration were considered. Two types of fumed silica nanoparticles (nonmodified and modified) were used to study the surface modification effect on agglomeration, void formation and gas separation properties of prepared membranes. Prepared nanocomposite membranes were characterized by scanning electron microscopy (SEM), thermal gravimetric analysis (TGA), Fourier transform infrared spectroscopy (FTIR) and tensile strength techniques. The gas permeabilities of hydrogen, methane, and carbon dioxide through pure PSf and nanocomposites were measured as a function of silica volume fraction, and permeability coefficients were determined using a variable pressure/constant volume experimental setup. Results showed that gas permeabilities increase with silica content, and proper H_2/CH_4 and H_2/CO_2 selectivities can be achieved with modified type of silica nanoparticles due to inhibition of particle agglomeration and bonding with polymer network. Hydrogen selectivity was improved by using 15 wt% polymer content instead of 9 wt% in preparation of nanocomposite membrane with same silica content. Gas permeation results indicated that increasing of feed pressure from 3 bar to 6 bar has a positive effect on selectivity of H_2/CH_4 but negligible effect on that of H_2/CO_2 for modified silica/PSf membrane.

Key words: Hydrogen Separation, PSf/SiO_2 Nanocomposite Membrane, Modification, Gas Permeation, Excess Free Volume

INTRODUCTION

In the membrane-based hydrogen separation processes, the separation performance strongly depends on the structural properties of the membrane used [1]. While glassy polymeric membranes have been extensively utilized for hydrogen separation applications, there is a trade-off between permeability and selectivity [2]. A new type of membrane material emerging with the potential for future applications is nanocomposite membranes composed of homogeneously interpenetrating polymeric and inorganic particle matrixes. Actually, it would be desired that the researchers could develop the new polymer/inorganic nanocomposite membranes with simultaneous improvement in both the permeability and selectivity. Therefore, we can pass from the limitation of neat glassy polymeric membranes.

For nearly a decade, the incorporation of inorganic particles such as porous zeolites [3-5], carbon nano tube [6-8], metal organic frame work [9-11], porous and nonporous silica [12-14] into a polymer matrix has been studied to enhance the ability of hydrogen separation membranes. However, the gas transport properties of nanocomposites are considerably affected by a variety of parameters, such as polymer and inorganic nanofillers, morphological characteristics, compatibility and absence of interfacial defects, and finally membrane preparation stage.

Polysulfone (PSf) is one of the most common glassy polymers that is widely used in many fields of separation like reverse osmosis (RO), ultrafiltration (UF) and gas separation (GS) [15]. Hydrogen can be separated effectively from H_2/CH_4 and H_2/CO_2 mixtures by selective permeation through PSf membranes. Besides ease of synthesis of silica, incorporation of these nanoparticles in polymer matrix can improve properties like mechanical, thermal and gas permeability of nanocomposite membranes [16-19].

There have been many attempts to incorporate silica nanoparticles in gas separation membranes.

Ahn et al. [20] prepared polysulfone (PSf)/silica nanocomposite membrane and investigated the effect of fumed silica nanoparticles on the gas separation performance of PSf membrane. They observed that the H_2 permeability of PSf/SiO_2 membrane with 20% vol.% of silica was 2.7 times greater than that of pure PSf. They also reported that H_2/CH_4 and H_2/CO_2 selectivities decreased from 53.6 and 1.87 in pure PSf to 29.36 and 1.64 in (20%) PSf/SiO_2 membrane, respectively. They showed that with addition of 20 vol% nonporous silica particles into the polysulfone matrix, an increase in the total free volume can be attained, and this leads to increase the diffusion and solubility coefficients of the silica filled polymer and causes an increase in the permeability of the penetrants.

Sadeghi et al. [21] studied the effect of silica nanoparticles on the gas separation performance of polybenzimidazole (PBI) membranes. PBI and PBI-silica hybrid membranes were prepared by thermal phase inversion method. They observed an enhancement in the solubility and a corresponding reduction in the diffusivity of the gases through the membranes by increasing the incorporation of

†To whom correspondence should be addressed.
E-mail: pakizeh@um.ac.ir

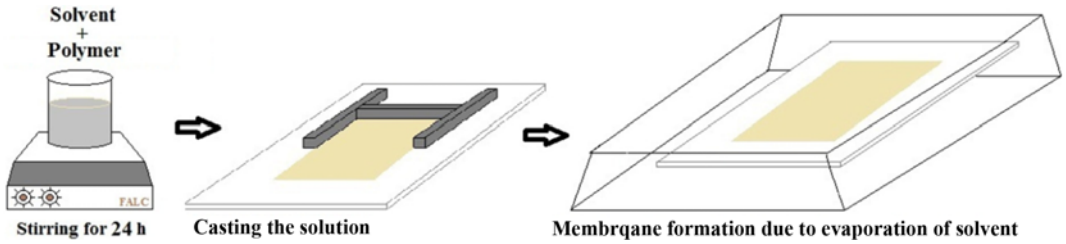

Fig. 1. Schematic represation of neat PSf membrane preparation.

nanoparticles in the polymer matrix. The permeability of the condensable CO_2 and CH_4 gases was increased upon increasing the silica content. The permeability of CO_2 and its selectivity over N_2 was increased from 0.025 barrer and 3.5 in pure PBI to 0.11 barrer and 71.3 in the PBI/silica nanocomposite containing 20 wt% of the silica particles.

Zornoza et al. [22] added mesoporous silica particles in PSF and compared mixed matrix membrane performance with pure PSF for gas separation. It was found from the results that 8 wt% filler loading was optimum for H_2/CH_4 selectivity (79.2). In addition, the permeability of H_2 and CH_4 increased with the increase in mass-% of silica loadings up to 32 wt% [23].

Gomes and coworkers [24] studied the gas separation properties of PTMSP/sol-gel derived silica nanocomposite membranes. They showed that the highest permeation properties of butane/methane were observed with silica content of 5.5 wt% in the polymer matrix.

Recently, Wahab and coworkers [25] studied the performance of PSf/fumed silica hollow fiber mixed matrix membranes for gas separation. They found that low loading of 0.1% (w/w) of fumed silica particles increased more than 12% in CO_2 permeability. The selectivities of CO_2/CH_4 and O_2/N_2 improved with an average value of 32.74 and 6.35, respectively. It has been also observed that at higher loading of 10% (w/w), permeation of slow gases (CH_4 and N_2) increased due to nanometric defects. Consequently, the selectivities of CO_2/CH_4 and O_2/N_2 were low at 7.43 and 2.02, respectively.

Particle agglomeration results in unselective voids formation at polymer-inorganic filler interface, which is the main problem related to nanocomposite membranes. Some attempts have been made to inhibit the particle agglomeration by introducing functional groups on the particle surface. In this research, as a new work, a comparative study has been conducted about effect of modification of silica particles as well as different polymer content on hydrogen separation performance and morphologies of prepared nanocomposites. Thus, permselectivities or ideal separation factors of pure PSf and nanocomposites membranes for H_2/CH_4 and H_2/CO_2 were measured via a variable pressure/constant volume membrane separation experimental setup. Permeabilities of hydrogen, methane and carbon dioxide gases were measured at 35 °C and feed pressures of 3 bar and 6 bar for prepared membranes with different silica content and the results were compared.

EXPERIMENTAL

1. Materials

Polysulfone (PSf(Ultrason-6010)) as polymer was supplied by BASF corporation for preparation of the membrane casting solutions. The fractional-free volume (FFV) of PSf is 0.16 as calculated by the Bondi group contribution method [26]. The reported density of PSf is 1.24 g/cm^3. Commercially, chloroform ($CHCl_3$), Dimethyldichlorosilane (DMDCS) and methanol were reagent grade and obtained from Merck. Deionized water was used for removing of casted films from glass plates. Nonporous silica nanoparticle known as S_1 with 7-14 nm average particle size was purchased from Plasma Chem of Germany and used as nanofiller. Hydrogen, carbon dioxide and methane were obtained from Technical Gas Services with high purity (99.99%).

2. Pure PSf Membrane Preparation

PSf powder was degassed and dried in a vacuum oven at 100 °C for 12 h and then dissolved in chloroform (9 and 15 wt%) under stirring (Heidolph model MR3001) for 24 h, and then prepared solution was filtered through a 0.45 μm pore size PTFE syringe filter. Casting was performed at room conditions using an accurate casting knife (Elcometer 3580). Polymer solution was cast at a designated wet thickness (200 μm) onto a clean and polished glass plate. The cast film on the flat glass was put in a closed with clean atmosphere homemade chamber immediately in order to slow evaporation of solvent. After 24 h, the prepared membrane was soaked in deionized water for separating of membrane from flat glass. The obtained membrane was dried at 80 °C in an oven for 12 h. The schematic representation of neat PSf membrane preparation is depicted in Fig. 1.

3. Silica Modification

Nanosilica was chemically modified through silanization reaction. As shown in Fig. 2, the silanol (Si-OH) groups on fumed SiO_2 are replaced by dimethylchlorosilane during surface modification. Fumed SiO_2 was immersed in DMDCS and stirred for 72 hr at room temperature. The modified SiO_2 was recovered from the solution through Soxhlet extraction apparatus using 250 ml of methanol. Modified SiO_2 product was labeled as S_2.

4. PSf/Silica Nanocomposite Membrane Preparation

The silica/PSf nanocomposite membranes were prepared by solution-casting route. Initially, a mixture of solvent and silica nanoparticles (S_1 or S_2) powder with known weight fraction was stirred for 24 h. The solvent/silica particle mixture was then sonicated (Hielscher model UP-400S) for 5 min in order for homogeneous distribution

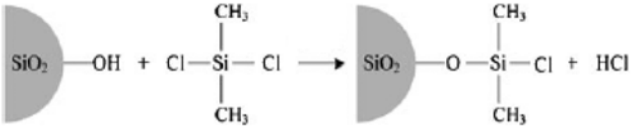

Fig. 2. Silanization reaction of fumed silica with DMDCS.

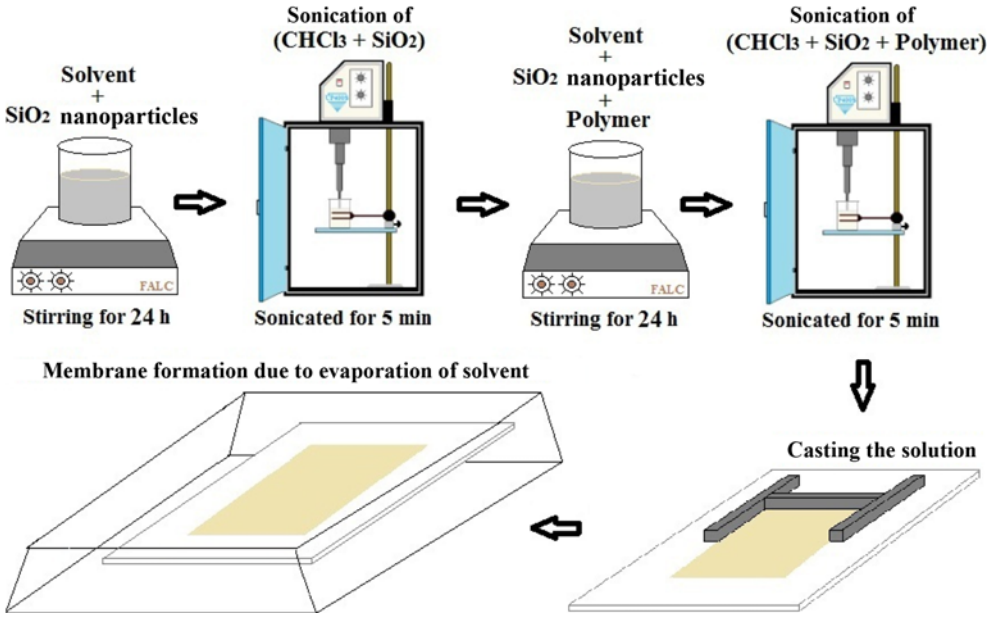

Fig. 3. The experimental procedures for nanocomposite preparation.

Table 1. Polymer weight fraction, silica type and silica volume fraction of prepared membranes

Membrane	M1	M2	M3	M4	M5	M6	M7	M8	M9	M10
wt% Polymer	9	15	9	9	9	9	15	15	15	15
Silica type	-	-	S_1	S_1	S_2	S_2	S_1	S_1	S_2	S_2
Silica content, %	0	0	10	25	10	25	10	25	10	25

of the silica nanoparticles in the solvent solution. PSf was degassed and dried in a vacuum oven, dissolved in chloroform (9 or 15 wt%) under stirring for 24 h and then filtered. At first, 10% of the polymer solution as a primer was added to the solution during 4 h to inhibit the agglomeration of nanoparticles. By this priming treatment, a thin layer of polymer surrounds outer surface of the silica particles and will lead to proper compatibility and avoiding defect forming between polymer and silica particles. Then the remaining polymer solution was added on the as-prepared solution slowly under stirring and stirred for 24 h. The polymer/silica particle solution mixture was then sonicated in order for homogeneous distribution of the silica nanoparticles in the polymer solution (The polymer and silica mixture was sonicated initially for 1 h and then left standing for 12 h). This procedure was repeated once for low silica loadings (10%), and two times for high silica loadings (25%) in the polymer solution. Twenty minutes before casting, the mixture was sonicated again for 1 h. The solution was cast on a flat glass plate and was slowly evaporated at room conditions for 24 h under closed chamber; then as obtained film was removed from the glass plate by soaking in deionized water. Finally, the nanocomposites films were dried at 80 °C for 24 h in vacuum oven to evaporate residual solvents. The silica content was calculated as volume fraction (Φ_f) by the following equation:

$$\phi_f = \frac{\omega_f/\rho_f}{\omega_f/\rho_f + \omega_p/\rho_p} \quad (1)$$

Where ω_f and ω_p refer to the weight of silica filler and polymer, respectively; also ρ_f and ρ_p are the density of filler and polymer, respectively. The thickness of membranes was measured by a micrometer and was typically in the range of 80-120 μm.

Fig. 3 shows the experimental procedures for nanocomposite preparation and the specifications of final prepared membranes are summarized in Table 1.

5. Characterizations

5-1. Scanning Electron Microscopy (SEM)

The membranes were fractured under liquid nitrogen to give a generally consistent and clean break. The membranes were then sputter-coated with thin film of gold and were mounted on brass plates with double-sided adhesive tape in a lateral position. Cross-sectional images of the membranes were obtained with a Philips SEM model XL30 microscope. The morphology of nonporous silica nanoparticles in PSf can be observed by SEM of freeze fractured specimens.

5-2. Thermo Gravimetric Analysis (TGA)

Residual solvent was removed from the test films by drying overnight in a vacuum oven at 70 °C. The thermal degradation was conducted by thermo gravimetric analysis (TGA) in Shimadzu (TGA-50/50h). About 2 mg of sample was loaded in a pre-tarred platinum pan and pre-heated above 120 °C to remove moisture. After cooling, the sample was reheated from 25 to 700 °C at a rate of 10 °C/min.

5-3. Fourier-transform Infrared Spectroscopy (FTIR)

FTIR (Thermo Nicolet Avatar 370) was used to characterize presence of functionalized groups in DMDCS modified silica, pure PSf and PSf/SiO_2 nanocomposite membranes. FTIR spectra were collected at wave number between 4,000 cm^{-1} to 400 cm^{-1} with spec-

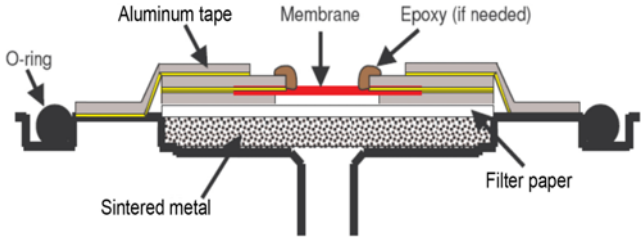

Fig. 4. Schematic representation of membrane cell used in this study.

tral resolution of 1 cm^{-1}.

5-4. Mechanical Strength Test

The tensile strength at break of selected membranes was obtained using a universal testing machine (ZWICK-Z250, Germany) by employing an extension rate of 5 mm/min at room temperature. Three membranes of each selected membrane were tested and then the average tensile strengths were reported.

5-5. Gas Permeation Measurement

The stainless steel dead-end membrane cell was used to perform the gas permeation experiments. The schematic view of manufactured membrane module is shown in Fig. 4. The membranes were housed in a cell that consisted of two detachable parts. Rubber O-rings were used to supply a pressure-tight seal between the membranes and the cells. The membrane had an effective area of approximately 11.34 cm^2.

The pure-gas (H_2, CH_4 and CO_2) permeation properties of PSf and PSf/silica nanocomposite membranes carried out using a constant volume/variable pressure experimental setup as shown in Fig. 5.

The gas permeability apparatus allows permeability to be determined by recording the increase of downstream pressure with time. The downstream and upstream parts of the membrane cell were evacuated by an oil-free vacuum pump prior to entering of the gases to the feed side of the module. The whole system was contained in a temperature-controlled oven and the experiments were performed at 35 °C. The upstream pressure was 3-6 bar and the initial downstream pressure was maintained at less than 15 mTorr. The single gas permeation tests were carried out from H_2 (the fastest) to CO_2, since the CO_2 is proven to cause plasticization effect on the membrane. The membrane selectivity was evaluated using the Eq. (2):

$$\alpha_{A/B} = \frac{P_A}{P_B} \tag{2}$$

Where P and α are gas permeability and permselectivity, respectively. Permeability, P, can be calculated by the following equation:

$$P = \frac{273.15 \times 10^{10} VL}{760AT\left(\frac{76 \times p_f}{14.7}\right)}\frac{dp}{dt} \tag{3}$$

Where V (cm^3) is the permeation cell volume, L is the membrane thickness (cm), dp/dt is the downstream gradient pressure (mmHg/s), p_f (psia) is the feed gas pressure, T (K) is temperature and A (cm^2) is the effective area of membrane. The gas permeability is commonly reported by the barrer unit (1 barrer=10^{-10} cm^3 (STP) cm/(cm^2 s cmHg)).

RESULTS AND DISCUSSION

1. Morphology

The dispersion of silica particles as well as PSf morphology dramatically influence the permeation properties of PSf/silica nanocomposite. Consequently, the distribution of added silica in continuous organic phase was studied by SEM taken at proper magnification. A cross section of pure PSf membranes at different polymer content (M1 and M2) can be observed in Fig. 6.

Clearly, one can see the increment of polymer content from 9% in M1 sample to 15% in M2 sample leads to tight morphology of M2 membrane. It is expected that this high dense structure leads to lowering of gas permeability.

The structure quality and size of S_1 agglomerated particles in M3 and M4 samples is presented in Fig. 7. As shown, the S_1 silica nanoparticles have been dispersed but appear to form agglomerates in the PSf matrix, and the agglomerate size increases at higher silica content. It can be observed that the agglomerate size reaches as high

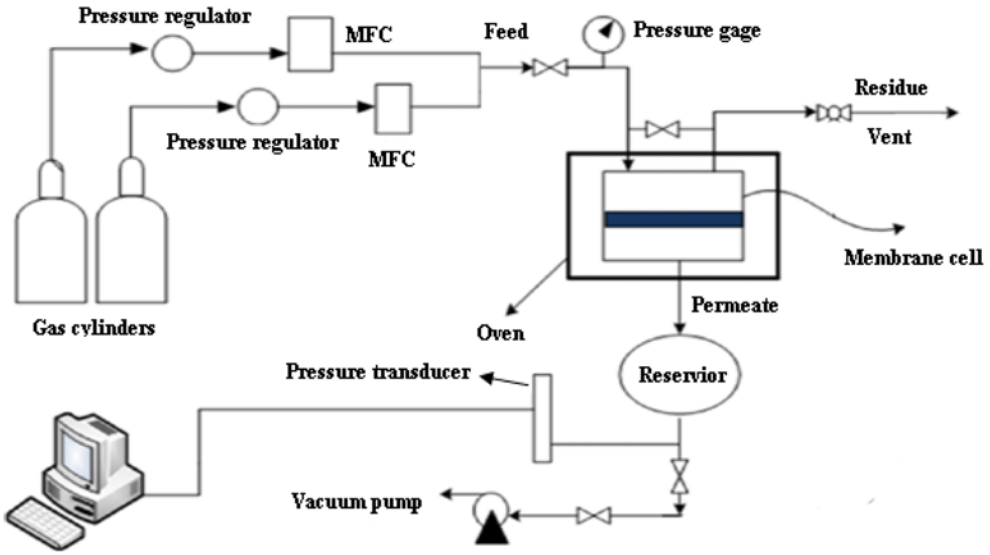

Fig. 5. Variable pressure/constant volume experimental set up for gas separation.

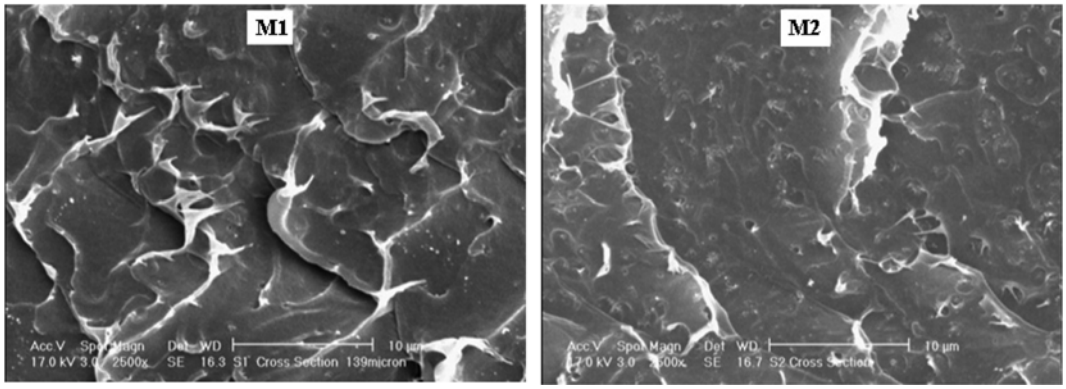

Fig. 6. Cross section of neat PSf membranes (M1; 9% PSf and M2; 15% PSf).

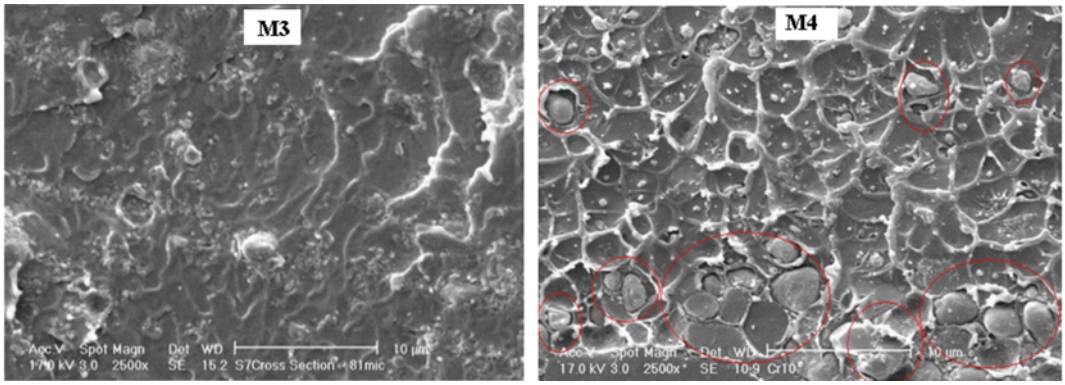

Fig. 7. Cross section of silica(S_1)/PSf membranes (M3; 5% silica and M4; 25% silica), both with 9% PSf.

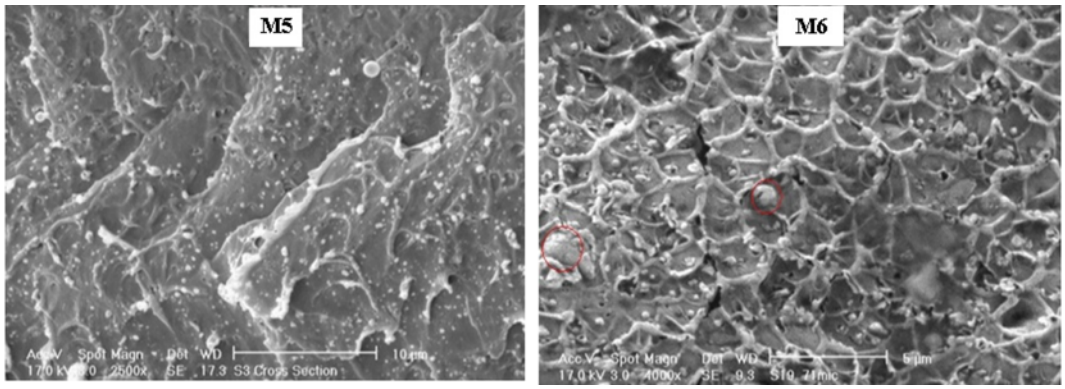

Fig. 8. Cross section of silica(S_2)/PSf membranes (M5; 10% silica and M6; 25% silica), both with 9% PSf.

as a few 2 μm (M4 sample). The SEM image shows that the spherical fumed silica particle cluster is embedded in the polymer matrix. However, it is simple to distinguish clearly the interfacial voids between the polymer network and silica particles, particularly in SEM of the M4 sample. Generally, because of the strong aggregation tendency of the hydrophilic fumed silica, fabricating of an ideal nanocomposite membrane with appropriate dispersion of nanoparticles is very difficult. The organic-inorganic interface defects can affect the membrane separation properties as will be discussed in the following section.

Fig. 8 shows the dispersion quality of S_2 type silica in M5 and M6 membranes which have been prepared at 9 wt% of PSf. As can be seen in the M5 sample, in contrast to the M4 sample the obvious voids are not detected due to proper distribution of silane modified nanoparticles into the polymer matrix. Pechar et al. [27] and Husain et al. [28] reported similar observations by using modified zeolite incorporated into polymer matrix in which zeolite filler was dispersed homogeneously in the prepared mixed matrix membranes. Actually, by modification process, the silane molecule can be reacted with the hydroxyl group attached to the surface of the silica particles.

Silanization of silica particles also results in hydrophobic surface and avoiding of segregation of the particles [29,30]. However, by increasing the silica content from 10% to 25%, the segregated parti-

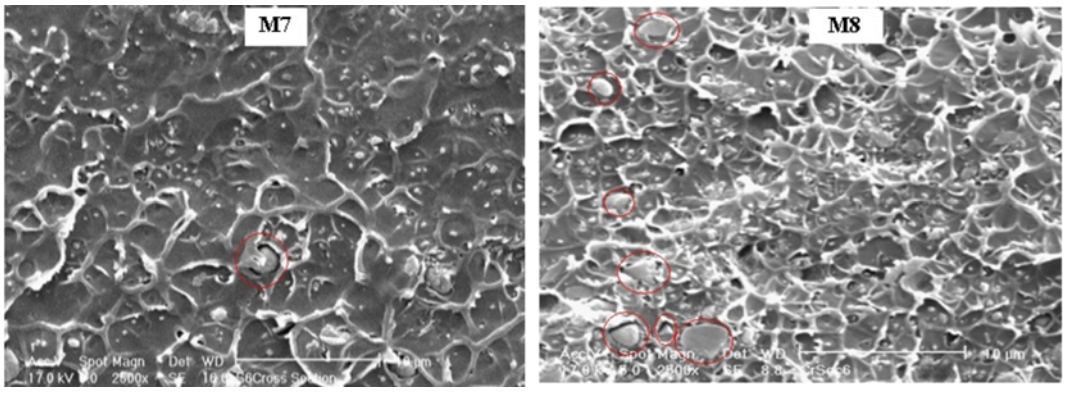

Fig. 9. Cross section of silica(S_1)/PSf membranes (M7; 10% silica and M8; 25% silica), both with 15 wt% PSf.

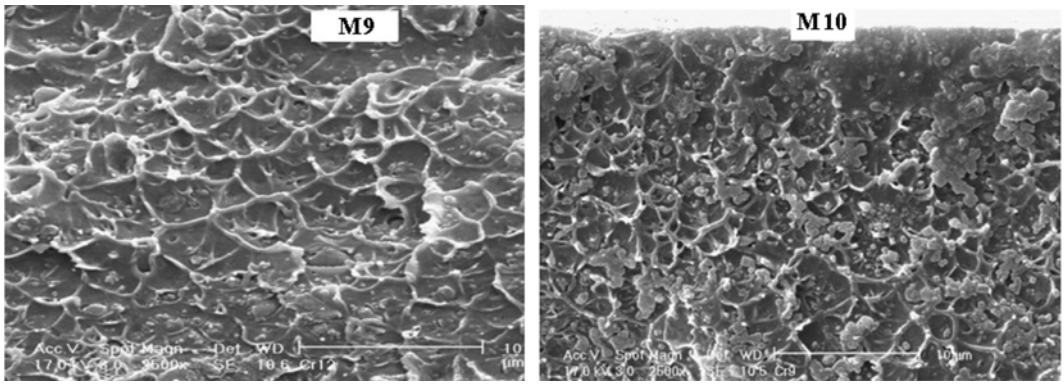

Fig. 10. Cross section of silica(S_2)/PSf nanocomposite membranes (M9; 10% silica and M10; 25% silica), both with 15 wt% PSf.

cle (at low level) even for modified silica in 9 wt% polymer can be shown in M6 membrane.

To study the effect of polymer concentration on the particle segregation, morphology and gas permeation properties, the nanocomposites with higher polymer content (15 wt%) were prepared and SEM images have been presented in Figs. 6, 9 and 10. As indicated in Fig. 8, for sample M6 with silica content of 25% and 9 wt% of PSf, a little extent of voids and segregation can be seen. Indeed, the nanocomposites membrane cast from solution with lower polymer concentration makes an inorganic rich region and a polymeric rich region due to low-viscosity of solution. Thus, for M10 sample with more viscous initial solution, one can detect clearly no existence of voids between the organic-inorganic phases and no presence of micronized-agglomerated particles in polymer matrix. Similar trend can be observed when we compare M4 and M8 samples with same 25% S_1 silica content.

2. Thermal Gravimetric Analysis (TGA)

The thermal properties of unfilled PSf and S_2 silica-filled PSf nanocomposites were studied by TGA analysis. The start decomposition temperature of the samples is observed at about 500 °C, as shown in Fig. 11. The initial weight loss is detected for pure PSf, which is mainly due to the removal of less volatile components of the PSf chain structure and adsorbed solvents. There is no sign of weight losses for hybrid PSf/silica membranes before degradation temperature. This behavior can be explained by the presence of modified silica nanoparticles in the polymer network, which cause the polysulfone to be thermally more stable at temperature range up to the decomposition temperature.

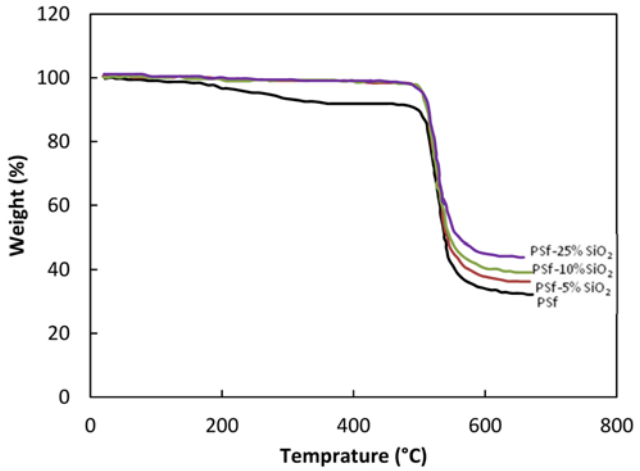

Fig. 11. Thermogravimetric analysis of nanocomposite and pure polysulfone samples in air with a heat-treatment of 10 °C/min.

3. FTIR

The FTIR spectra of silica nanoparticles and PSf based membranes are depicted in Figs. 12 and 13. According to Fig. 12, the nonmodified silica nanoparticles show band of O-Si-O at 1,101 cm^{-1}, and two bands due to presence of the silanol groups including 3432 (Si-OH stretching) and 1,627 cm^{-1} (Si-OH bending). The band at 811 cm^{-1} corresponds to -OH stretching vibration. Modification of S_1

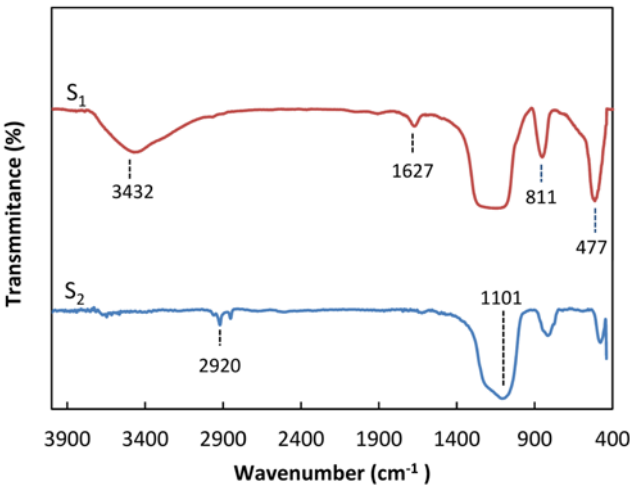

Fig. 12. The FTIR spectra of silica nanoparticles.

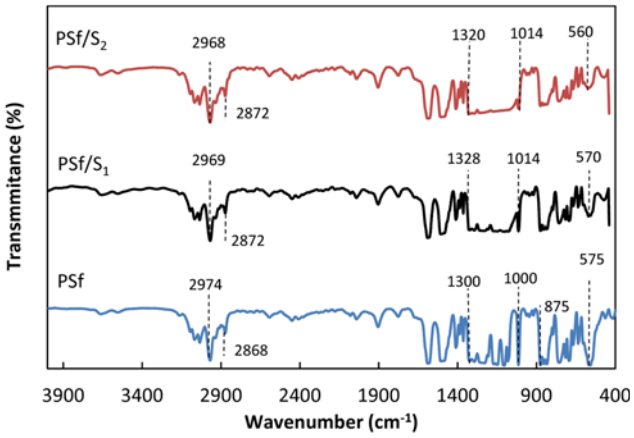

Fig. 13. The FTIR spectra of neat PSf and nanosilica embedded PSf membranes.

Table 2. Tensile strength of pure PSf and PSf/silica nanocomposite membranes

Membrane code	Tensile strength (MPa)	standard deviation
M2	47.33	0.83
M7	52.25	1.35
M9	61.64	2.12

Table 3. Molecular gas properties [38]

Gas molecule	Critical temperature (K)	Kinetic diameter, d_k (Å)
H_2	33.2	2.89
CO_2	304.2	3.3
CH_4	190.6	3.8

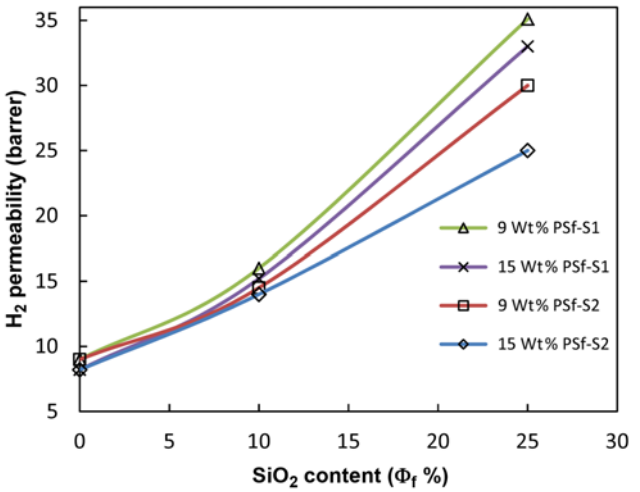

Fig. 14. H_2 permeablity (barrer) of pure PSf and PSf/SiO_2 nanocomposite membranes at T=35 °C and P_f of 3 bar.

nanosilica with DMDCS confirms a new band at 2,920 cm^{-1} related to the C-H asymmetrical stretching vibration. Also, the intensity of the bands at about 1,627 and 3,370 cm^{-1} is reduced due to reduction of silanol groups [31,32].

Fig. 13 compares the FTIR spectrum of PSf/S_2, PSf/S_1 and neat PSf membranes. For neat PSf membrane two bands occur at 1,229 cm^{-1} and 1,295 cm^{-1}, which is associated with the symmetric O-S-O stretching vibration. The band at 2,974 cm^{-1} is attributed to the asymmetric -CH_3 stretching vibration band. Two bands of aromatic C-H and OH bond are shown at the wavenumbers of 2,868 cm^{-1} and about 3,600 cm^{-1}, respectively. The bands at 1,588-1,400 cm^{-1} region are due to the benzene ring skeletal stretching mode [33,34]. The band at 575-875 cm^{-1} became weaker for PSf/S_2 and PSf/S_1 nanocomposite membrane. Moreover, the bands at 1,010-1,290 cm^{-1} region are broader for PSf/S_2 than the pure PSf and PSf/S_1, which is related to the overlapping of the band of vibration of a sulfone group and Si-O-Si. According to Fig. 13, the polymer band shifts a little for nanocomposite PSf/Silica membrane, proposing existence of interaction between polymer and nanoparticles [35-37].

4. Mechanical Strength

The tensile strength of pure PSf and nanocomposite membranes is shown in Table 2. According to results one can conclude that the addition of nanosilica causes an increase in tensile strength of PSf membranes. As nanosilica is dispersed in polymer matrix, the free motion of polymeric chains is restricted by nanoparticles and tensile strength of membranes is enhanced consecutively. Nanoparticles-polymer interaction, uniform dispersion, and no agglomeration of nanoparticles lead to higher tensile strength. Comparing tensile strength data of PSf/S_2 and PSf/S_1 nanocomposite membrane confirms that modified silica interacts better with polymer chains.

5. Single Gas Permeation

Based on the obtained gas permeation data for pure PSf, the effects of silica nanoparticles in the PSf matrix and also polymer content on the gas permeation properties of prepared nanocomposites have been evaluated. The single gases tested include H_2, CH_4 and CO_2 which their molecular dimensions presented in Table 3 [38]. Based on kinetic diameter, the molecular dimension increases from H_2, CH_4 to CO_2. Fig. 14 presents the permeabilities of unfilled PSf and silica-filled PSf nanocomposite membranes with varying silica volume fraction (Φ_f), silica type and polymer content at 35 °C and feed pressure of 3 bar, respectively. The permeability of H_2 increased as the loading of nonporous silica increased at constant temperature

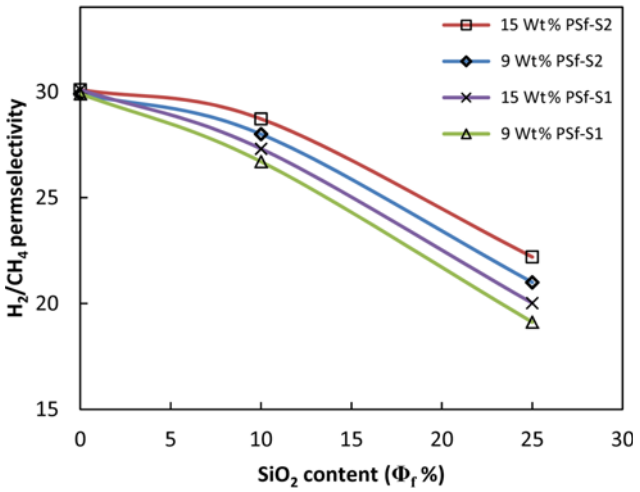

Fig. 15. H_2/CH_4 permselectivity of pure PSf and PSf/SiO_2 nanocomposite membranes at T=35 °C and P_f of 3 bar.

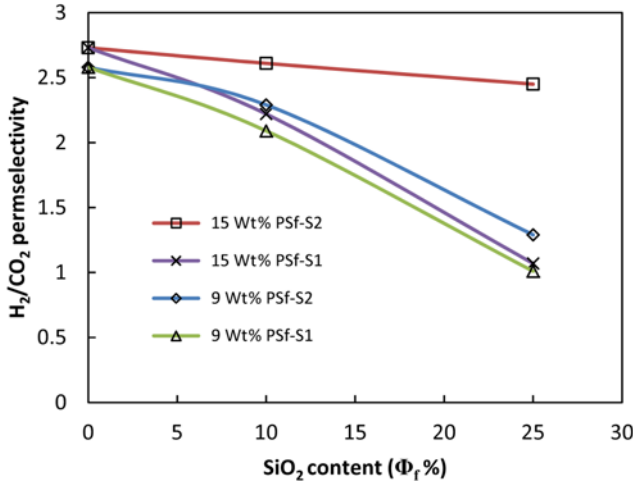

Fig. 16. H_2/CO_2 permselectivity of pure PSf and PSf/SiO_2 nanocomposite membranes at T=35 °C and P_f of 3 bar.

and feed pressure. In addition, Figs. 15 and 16 compare the selectivity results of H_2/CH_4 and H_2/CO_2 graphically.

As shown in Fig. 14, with addition of 25% S_1 silica to 9 wt% PSf membrane, H_2 permeability increased from 9 barrer for pure PSf membrane to 35.1 barrer. On the other hand, Fig. 15 and Fig. 16 demonstrate that H_2/CH_4 selectivity of 29.91 and H_2/CO_2 selectivity of 2.58 in pure PSf membrane decreased to 19.12 and 1.29, respectively. Similar trend can be observed for 15 wt% PSf-based membranes. These variations are due to the existence of S_1 silica/polymer voids in membrane that were already observed in SEM images of M4 and M8 samples (Figs. 7 and 9). In this case, gas molecules pass through the less resistant interfacial macro voids instead of passing through polymer intersegmental sites, and thus the separation properties of the nanocomposite membranes decreased. In fact, in preparation of an ideal PSf/silica nanocomposite, one must try to keep the concentrations of these nonselective voids at minimum level, but application of the methods which increase the polymer free volume is ordered.

Regarding Figs. 14 to 16, PSf/ S_2 silica nanocomposite membrane shows a slight decrease in H_2 permeability and a proper improvement on both H_2/CH_4 and H_2/CO_2 selectivities in comparison to S_1 PSf/silica nanocomposite membranes. As mentioned earlier, the modification of silica particles surface results in low aggregation of particles as well as bonding the particle surface to the polymer chain. This improvement in selectivity is consistent with the observed structure of M6 sample by SEM in Fig. 7, which indicates very low content of agglomerated particles and void between particles and polymer matrix. Polymer concentration effect on transport properties of prepared nanocomposites can be verified by considering the obtained permeation results in 9 wt% and 15 wt% PSf samples, which both group have same content of S_2 type silica. One can see, by increment of polymer content from 9 wt% to 15 wt%, that the H_2 permeability decreased. Similar trend can be nearly seen for M1 (9 wt%) and M2 (15 wt%) pure PSf membranes. Moreover, the H_2/CH_4 selectivity slightly increased while increase in the H_2/CO_2 selectivity was more intense. As an interesting result, it can be mentioned that PSf/ S_2 nanocomposite membrane containing higher polymer (15 wt%) is more suitable for H_2/CH_4 and H_2/CO_2 separation because of simultaneous high H_2 permeability and selectivity than other samples. When we compare the permeation data of M4 and M10 samples, it is realized that proper H_2/CH_4 and H_2/CO_2 selectivities can be achieved with S_2 type silica/PSf nanocomposite in which polymer content is 15 wt% (M10). In other words, among all samples, the M10 sample showed the best hydrogen separation performance and this can be described as that in higher polymer concentration probability of silica particle-polymer collusions is higher than particle-particle collusions; consequently, the aggregation of particles is restricted by organic phase. In this case the gas permeation is controlled only by created excess free volume due to qualified dispersion of S_2 silica nanoparticles into the polymer matrix and not to macroscopic voids which strongly decline the selectivity.

However, it is noticeable that nonporous nanosized S_2 silica disrupts polymer chain packing, leading to an increase in free volume in low-free-volume PSf glassy polymer.

Generally, polymer permeability property depends on molecular packing in the amorphous state. The diffusion of gas molecules is dependent upon the available free volume in the polymer matrix. Matteucci et al. [39] proposed the presence of free volume within a polymer. They defined free volume as that contribution to polymer-specific volume not occupied by the actual molecules. This may include small interstitial volume, which is distributed uniformly throughout the polymer, and excess free volume consisting of intersegmental defects large enough to allow gas molecule diffusion. Correlations of diffusion coefficients with free volume have been presented by researchers in the literature. Cohen and Turnbull [40] introduced a simplistic description of small molecule diffusion in glassy polymers, assuming the polymer can be described as a collection of hard spheres in a liquid-like state.

$$D_M = A\exp\left(\frac{-\gamma V^*}{V_f}\right) \quad (4)$$

Where A is a pre-exponential factor that depends weakly on temperature, and V_f is the average polymer free volume, which can be estimated from the polymer density and group contribution theory [41]. D decreases exponentially with increasing penetrant size (γV^*), which is consistent with experimental observation for penetrant dif-

Table 4. Effect of pressure on H_2 permeability (barrer), H_2/CH_4 and H_2/CO_2 permselectivity of 15 wt% pure PSf and PSf/modified-SiO_2 nanocomposite membranes at T=35 °C

Feed pressure (bar)	SiO_2 Φ_f%	H_2 permeability (barrer)	H_2/CH_4	H_2/CO_2
3	0	8.20 (±0.04)	30.10 (±0.03)	2.73 (±0.04)
	10	14.00 (±0.07)	28.72 (±0.04)	2.61 (±0.03)
	25	25.00 (±0.06)	22.20 (±0.05)	2.45 (±0.01)
6	0	8.00 (±0.03)	29.70 (±0.05)	2.68 (±0.01)
	10	18.10 (±0.05)	31.40 (±0.07)	2.55 (±0.05)
	25	30.70 (±0.04)	25.60 (±0.01)	2.45 (±0.02)

fusion at infinite dilution in glassy polymers. To prevent double counting of free volume elements shared by more than one hard sphere γ is introduced as an overlap parameter [41]. Although this model has a simple form, it shows the approximate dependence of the diffusion coefficient on the average free volume and we use it in explanation of the gas permeation results for S_2 silica/PSf nanocomposite membrane.

The influence of feed pressure on H_2 permeability and H_2/CH_4 and H_2/CO_2 selectivities of pure PSf and nanocomposites membranes has been shown in Table 4. In the case of pure PSf membranes increasing pressure from 3 bar to 6 bar leads to slight declining of permeability of gases. This can be described by saying that for glassy polymers the dual sorption model (DSM) predicts a decrease in permeability with increasing pressure. This trend has been confirmed for pure glassy polymers by other studies [42].

In contrast to pure PSf membranes, in the case of PSf/S_2 nanocomposites, the hydrogen permeability and H_2/CH_4 selectivity simultaneously increase with feed pressure, while the H_2/CO_2 selectivity does not show this behavior and approximately remains unchanged. This is because permeation behaviors of H_2 and CO_2 through the PSf/SiO_2 nanocomposites in high pressure are identical and differ from that of CH_4.

As a result, increase of upstream pressure favors the H_2/CH_4 separation, but this is not the case for that of H_2/CO_2. Based on reported studies in literature, hydrogen and methane are low sorbing molecules which must penetrate through the created excess free volume, whereas the CO_2 molecules have a tendency to condense on polymer. Therefore, by increasing pressure, small molecules (H_2) can penetrate faster than large molecules (CH_4) through the created excess free volume in nanocomposites; on the other hand CO_2 permeability will increase due to the increase in its solubility and not for diffusivity. Consequently, the H_2/CH_4 selectivity increases but H_2/CO_2 selectivity remains approximately constant with feed pressure.

Figs. 17(a) and (b) illustrate H_2/CH_4 and H_2/CO_2 selectivity against permeability of H_2 to evaluate the performance of PSf/S_2 and PSf/S_1 nanocomposite membranes. PSf as a low-free-volume glassy polymer has relatively low permeability and high selectivity. These polymer properties can be changed by the addition of nanofiller in polymer matrix. According to Fig. 17, PSf containing 25% of S_2 silica, the H_2 permeability increases about 3-fold, while the H_2/CH_4 and H_2/CO_2 selectivity decreases by 26.2% and 10%, respectively. The H_2 permeability results of PSf/S_1 (25% silica) nanocomposite membrane increase 4-fold and the H_2/CH_4 selectivity decrease about 33.49%. It is also observed that the H_2/CO_2 selectivity decreases

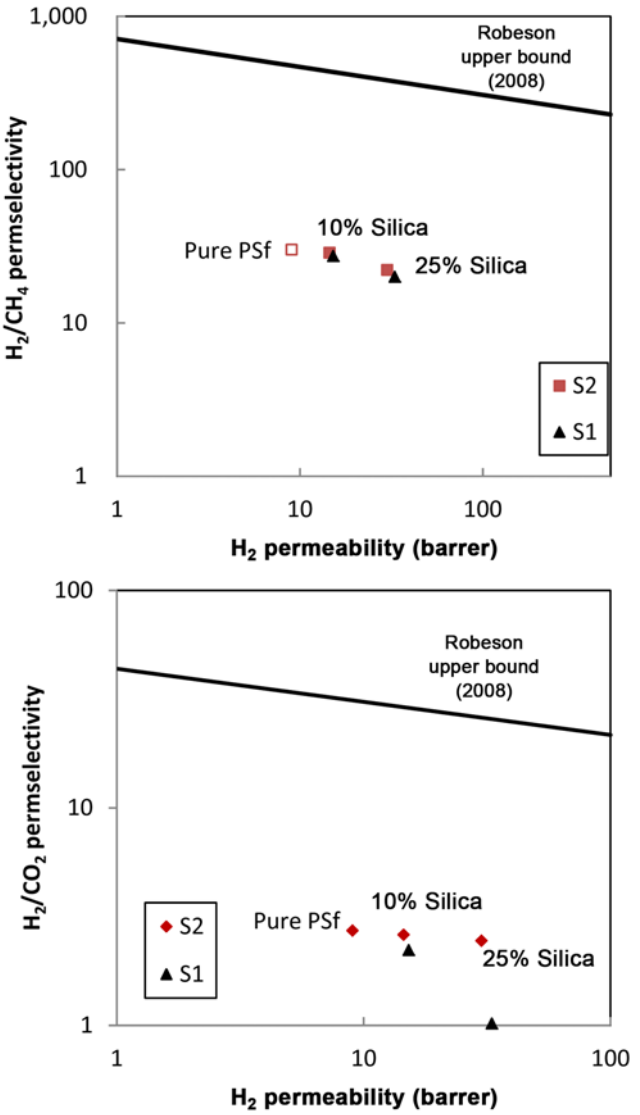

Fig. 17. Trade-off between H_2 permeability, H_2/CH_4 and H_2/CO_2 selectivity of PSf and PSf/silica nanocomposite membranes.

62.6%, which is noticeable compared with that of PSf/S_2 (25%) results. Although in the present study the new obtained selectivity versus permeability data does not overcome Robeson's upper bound [2], but it has been tried to investigate the effect of incorporation of modified and nonmodified fumed silica into polymer matrix on the performance of PSf membrane.

CONCLUSIONS

Different glassy pure polysulfone and PSf/silica nanocomposite membranes were successfully prepared. To investigate the effects of preparation parameters on the morphology and gas transport, various parameters including nanofiller content, surface modification and polymer concentration were considered. The addition of silica significantly enhances the gas permeability of polysulfone with increasing silica content. This behavior may result from unfavorable voids formation between agglomerated silica particles or an increase in free volume of PSf membrane.

Using surface modification of particles by coupling agent leads to inhibition of particle segregation and elimination of macro voids and proper attachment of silica particles to polymer network. The permeability of large gases through the unmodified PSf/silica membrane is more affected by the addition of silica resulting from the formation of voids. These voids significantly enhance the permeability and result in a reduction in pure-gas selectivity. In the case of modified PSf/silica membrane, the simultaneous improvement in hydrogen permeability and selectivity can be attained since the permeation is controlled through the increased free volume and not through the voids. Increase of polymer concentration reduces the void formation due to higher probability of particle-polymer collisions than particle-particle collisions and consequently affects gas permeation properties of nanocomposites in a desired direction. Increasing the upstream pressure favors the H_2 permeability as well as H_2/CH_4 selectivity but has no meaningful influence on H_2/CO_2 selectivity.

ACKNOWLEDGEMENTS

The authors are grateful for the financial support provided by the Iran National Science Foundation (INSF) and Ferdowsi University of Mashhad under grant number of 35462.

REFERENCES

1. L. Shao, C.-H. Lau and T-S. Chung, *Int. J. Hydrog. Energy*, **34**, 8716 (2009).
2. L. M. Robeson, *J. Membr. Sci*., **320**, 390 (2008).
3. Z. Huang, Y. Li, R. Wen, M. M. Teoh and S. Kulprathipanja, *J. Appl. Polym. Sci*., **101**, 3800 (2006).
4. G. Golemme, A. Bruno, R. Manes and D. Muoio, *Desalination*, **200**, 440 (2006).
5. D. Li, H. Yong Zhu, K. R. Ratinac, S. P. Ringer and H. Wang, *Micropor. Mesopor. Mater*., **126**, 14 (2009).
6. S. Kim, T. W. Pechar and E. Marand, *Desalination*, **192**, 330 (2006).
7. S. Kim, L. Chen, J. K. Johnson and E. Marand, *J. Membr. Sci*., **294**, 147 (2007).
8. T.-H. Weng, H.-H. Tseng and M.-Y. Wey, *Int. J. Hydrog. Energy*, **34**, 8707 (2009).
9. A. Car, C. Stropnik and K. V. Peinemann, *Desalination*, **200**(1-3), 424 (2006).
10. Y. Zhang, I. H. Musselman, J. P. Ferraris and K. J. Balkus, *J. Membr. Sci*., **313**(1/2), 170 (2008).
11. T. Yang, Y. Xiao and T. S. Chung, *Energy Environ. Sci*., **4**, 4171 (2011).
12. Y. K. Vijay, N. K. Acharya, S. Wate and D. K. Avasthi, *Int. J. Hydrog. Energy*, **28**, 1015 (2003).
13. L. Shao and T. S. Chung, *Int. J. Hydrog. Energy*, **34**, 6492 (2009).
14. V. Bhardwaj, A. Macintosh, I. D. Sharpe, S. A. Gordeyev and S. J. Shilton, *N. Y. Acad. Sci*., **984**, 1 (2003).
15. R. W. Baker, *Membrane technology and applications*, 2nd Ed., John Wiley & Sons, Ltd., New York (2004).
16. T. S. Chung, L. Y. Jiang, Y. Li and S. Kulprathipanja, *Prog. Polym. Sci*., **32**, 483 (2007).
17. G. Brusatin, G. D. Giustina, M. Guglielmi, M. Casalboni, P. Prosposito, S. Schutzmann and G. Roma, *Mater. Sci. Eng. C*, **27**, 1022 (2007).
18. Y. W. Wang, C. T. Yen and W. C. Chen, *Polymer*, **46**, 6959 (2005).
19. W. J. Koros and R. Mahajan, *J. Membr. Sci*., **175**, 181 (2000).
20. J. Ahn, W. J. Chung, I. Pinnau and M. D. Guiver, *J. Membr. Sci.*, **314**, 123 (2008).
21. M. Sadeghi, M. A. Semsarzadeh and M. Moadel, *J. Membr. Sci*., **331**, 21 (2009).
22. B. Zornoza, S. Irusta, C. Tellez and J. Coronas, *J. Langmuir*, **25**, 5903 (2009).
23. T. Kono, Y. Hu, T. Masuda, K. Tanaka, R. D. Priestley and B. D. Freeman, *Polym. Bull*., **58**, 995 (2007).
24. D. Gomes, S. P. Nunes and K. V. Peinemann, *J. Membr. Sci*., **246**, 13 (2005).
25. M. F. A. Wahab, A. F. Ismail and S. J. Shilton, *Sep. Purif. Technol*., **86**, 41 (2012).
26. A. Bondi, *J. Phys. Chem.*, **68**, 441 (1964).
27. T. W. Pechar, S. Kim, B. Vaughan, E. Marand, M. Tsapatsis, H. K. Jeong and C. J. Cornelius, *J. Membr. Sci*., **277**, 195 (2006).
28. S. Husain and W. J. Koros, *J. Membr. Sci*., **288**, 195 (2007).
29. Y. Li, H. M. Guan, T. S. Chung and S. Kulprathipanja, *J. Membr. Sci*., **275**, 17 (2006).
30. J. Duval, A. Kemperman, B. Folkers, M. Mulder, G. Desgrandchamps and C. Smolders, *J. Appl. Polym. Sci*., **54**, 409 (1994).
31. Y. Xu, Z. H. Li, W. H. Fan, D. Wu, Y. H. Sun, L. X. Rong and B. Z. Dong, *Appl. Surf. Sci*., **225**, 116 (2004).
32. L. Wang, A. Lu, Z. Xiao, J. Ma and Y. Li, *Appl. Surf. Sci.*, **255**, 7542 (2009).
33. D. Ficai, A. Ficai, G. Voicu, B. S. Vasile, C. Guran and E. Andronescu, *Materiale Plastice*, **47**, 24 (2010).
34. M. A. Elharati, *Poly(vinyl alcohol)/polyamide thin-film composite membranes*, Thesis for the degree of Master of Science in Engineering, Stellenbosch University (2009).
35. F. Dorosti, M. R. Omidkhah, M. Z. Pedram and F. Moghadam, *Chem. Eng. J.*, **171**, 1469 (2011).
36. L. Mingliang, W. Qingzhi, L. Jialin, L. Hongjian and J. Zilong, *Chinese J. Chem. Eng*., **19**, 45 (2011).
37. V. Vatanpour, S. S. Madaeni, L. Rajabi, S. Zinadini and A. Ashraf Derakhshan, *J. Membr. Sci*., **401**, 132 (2012).
38. Y. Yampolskii, I. Pinnau and B. D. Freeman, *Materials science of membranes for gas and vapor separation*, John Wiley & Sons, Ltd., New York (2006).
39. S. Matteucci, Y. Yampolskii, B. D. Freeman and I. Pinnau, *Transport of gases and vapors in glassy and rubbery polymers*, In: Y. Yampolskii, I. Pinnau, B. D. Freeman (Eds.), Membranes for Gas and Vapor Separation, Wiley, Chichester, 6-14 (2006).
40. M. Cohen and T. Turnbull, *J. Chem. Phys*., **31**, 1164 (1959).
41. A. Bondi, *Physical properties of molecular crystals, liquids and gases*, John Wiley & Sons. Inc., New York (1968).
42. V. T. Stannett, *J. Membr. Sci*., **3**, 97 (1978).